

Lawrence Berkeley National Laboratory

Recent Work

Title

ORDERED S-MATRIX APPROACH TO THE TOPOLOGICAL EXPANSION FOR BARYONS AND MESONS

Permalink

<https://escholarship.org/uc/item/0vq5k8zr>

Author

Stapp, Henry P.

Publication Date

1977-08-01

UC-34d
LBL-6735 (v.1)

RECEIVED
PHYSICS DEPARTMENT
UNIVERSITY OF CALIFORNIA
BERKELEY
AUG 17 1977
DEBAR AND
PHYSICS DEPARTMENT

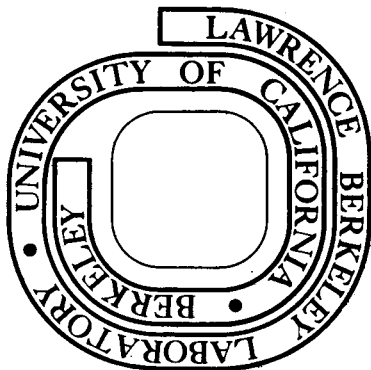
ORDERED S-MATRIX APPROACH TO THE TOPOLOGICAL
EXPANSION FOR BARYONS AND MESONS

For Reference

Not to be taken from this room

Henry P. Stapp

August 16, 1977



Prepared for the U. S. Department of Energy
under Contract W-7405-ENG-48

DISCLAIMER

This document was prepared as an account of work sponsored by the United States Government. While this document is believed to contain correct information, neither the United States Government nor any agency thereof, nor the Regents of the University of California, nor any of their employees, makes any warranty, express or implied, or assumes any legal responsibility for the accuracy, completeness, or usefulness of any information, apparatus, product, or process disclosed, or represents that its use would not infringe privately owned rights. Reference herein to any specific commercial product, process, or service by its trade name, trademark, manufacturer, or otherwise, does not necessarily constitute or imply its endorsement, recommendation, or favoring by the United States Government or any agency thereof, or the Regents of the University of California. The views and opinions of authors expressed herein do not necessarily state or reflect those of the United States Government or any agency thereof or the Regents of the University of California.

ORDERED S-MATRIX APPROACH TO THE TOPOLOGICAL
EXPANSION FOR BARYONS AND MESONS*

Henry P. Stapp

Lawrence Berkeley Laboratory
University of California, Berkeley, California 94720

August 16, 1977

ABSTRACT

A proposal is made for extending to processes involving baryons the ordered Hilbert space approach to the topological expansion. The proposal is based on a topological classification scheme for baryonic processes that is similar to one used previously for the lowest-order contributions, but is in terms of the minimum number of reggeon closed loops instead of handles.

* This work is supported by the U. S. Energy Research and Development Administration under the auspices of the Division of Physical Research.

1. Introduction

To perform reliable calculations in strong-interaction physics one needs an approximation scheme in which the lowest order term is already a fairly good approximation, and the higher-order corrections fall off rapidly. The main idea for such a scheme has been set forth by Veneziano¹ under the title "topological expansion." Veneziano's idea is that contributions to scattering amplitudes should be represented graphically, and that these graphs should be grouped in accordance with their genus, which is the number of handles on the surface of fewest handles upon which the graph can be imbedded in a locally planar fashion.² Various arguments have been given for expecting the suppression of graphs of higher genus, and calculations based on this expectation seem to work reasonably well.³

The lowest-order term in the topological expansion had originally been conceived to be an appropriate dual amplitude. However, no dual amplitude has been found that is both mathematically and physically acceptable. Veneziano's recent works⁴ have focused rather on the possibility that quantum chromodynamics might provide a framework for unifying various lines of development in strong interaction physics. The expansions he considers in this connection are not strictly topological, but are expansions in the inverses of the numbers of flavors and colors in various combinations.

Other workers have been calculating characteristics of Regge parameters based on a combination of S-matrix ideas and topological considerations.⁵ These efforts have pointed to the need

5037084807305

for a formulation of the topological expansion that does not rely either on the existence of an acceptable dual-model starting point, or upon the solubility of quantum chromodynamics.

Recently Chew, Lucht, and Weissmann⁶ have proposed an approach to the topological expansion based on the concept of an ordered S-matrix. Their proposal, which deals specifically with the meson sector, is based on the introduction of a new Hilbert space in which the particles are linearly ordered. That is, each state of a basic orthonormal set of states is labelled by an ordered sequence of particle labels:

$$|\psi\rangle = |p_1, \mu_1, t_1; p_2, \mu_2, t_2; \dots, p_n, \mu_n, t_n\rangle.$$

Here the set (p_i, μ_i, t_i) specifies the momentum-energy, the spin component, and the particle-type of the i^{th} particle in the state $|\psi_\alpha\rangle$. Ordinarily the state $|\psi'_\alpha\rangle$ obtained by interchanging (p_i, μ_i, t_i) with (p_j, μ_j, t_j) is equal to the original state up to a possible phase. But in the ordered Hilbert space this change of ordering yields a new state that is orthogonal to the original one unless $(p_i, \mu_i, t_i) = (p_j, \mu_j, t_j)$.

This new Hilbert space is not the usual one. But Chew, Lucht, and Weissmann consider the possibility of constructing in this new Hilbert space a unitary S-matrix that satisfies the usual S-matrix analyticity requirement that it have only those singularities demanded by unitarity. One can then follow through the usual S-matrix arguments that lead to cluster decomposition,

crossing, and singularity structure.⁷ The ordering of the particles of the basic vectors of the Hilbert space induces a cyclic ordering of the particles associated with each scattering function. That is, each scattering function (which is the analytic function corresponding to the connected part of the S-matrix) is specified by giving both a set of particles and a specific cyclic ordering of these particles. These amplitudes are called ring amplitudes, and they are represented graphically by a circle or ring drawn on a plane with the particle lines attached in the specified cyclic order (See Fig. 1). The singularities possessed by a given ring amplitude include only those singularities that correspond to Landau diagrams that can be drawn as planar diagrams inserted into the ring diagram. A typical Landau diagram corresponding to the ring diagram of Fig. 1 is shown in Fig. 2.

The ring amplitude is analogous to the ordered planar contribution in Veneziano's topological expansion. But here it is considered to be defined by the unitarity and analyticity properties stemming from the ordered Hilbert space. Thus the pole-factorization property entailed by unitarity and by the general analyticity assumption (macrocausality) must hold. And there must be complete consistency between the internal poles of the ordered amplitude and the particles that define the ordered Hilbert space. Thus the ring amplitudes, which are the fundamental building blocks of the theory, are defined neither by some yet-to-be discovered dual model, nor by the infinite sum of planar contributions to some field theoretic model, but rather as the assumed self-consistent solution of the ordered S-matrix equations.

These equations are much simpler than the full S-matrix equations because the analytic structure is much simpler: the only singularities of a ring function are those corresponding to a particular set of planar Landau diagrams.

With the ring amplitudes considered as given one can proceed with the construction of the physical amplitudes. The first step is to define a "planar amplitude" corresponding to each given set of particles. This planar amplitude is defined to be the sum of the ring amplitudes over all of the different cyclic orderings of the given set of particles. This planar amplitude is considered to be the first approximation to the physical scattering amplitude.

The different orders of approximation are defined by means of a topological classification scheme. Each planar amplitude is, as just stated, a sum of ring amplitudes. Thus in a unitarity product of planar amplitudes one will encounter various products of two ring amplitudes. And in higher order calculations one will encounter similar unitarity-type products of many ring amplitudes. A typical product involving four ring amplitudes is indicated diagrammatically in Fig. 3. An equivalent, but more compact representation is shown in Fig. 4.

One must now determine the genus of a graph such as the one of Fig. 4. The theory of the minimal imbedding of a graph on a surface has been given by J. W. T. Youngs⁸. Youngs shows that a minimal imbedding (i. e., an imbedding on a surface with a minimum number of handles) is necessarily a two-cell imbedding. This

means that if S is a surface upon which G is minimally imbedded then each component (connected part) of S - G is topologically equivalent to a disc. That is, each connected part of S minus G resembles a connected open portion of a planar surface.

For any two-cell imbedding the Euler formula holds. This formula

$$(1.1) \quad 2h = 2 + E - V - F$$

says that twice the number of handles, 2h, is two plus the number E of edges of G minus the number V of vertices of G minus the number F of faces of S - G. The faces of S - G are the components (connected parts) of S - G.

In graph theory each edge runs between two vertices, and hence one should, in principle, place vertices on the ends of the external lines. However, one can ignore these external vertices in equation (1.1) if one ignores also the external lines. Thus we shall consider the graph of Fig. 4 to have V = 4 and E = 6.

The number of faces F can be computed by a simple procedure. One places a point on one side of a line of G and then traces a path that stays always next to a line of G, and at each vertex moves continuously to a unique adjacent side of a unique adjacent line. This unique side of a unique line is determined by the condition that the path cross no line that is attached to the vertex. The path is traced out in this way until it returns to the original starting point. This path lies near

09004807306

the boundary of a single face. An example is shown in Fig. 5. (The detours around the external lines should have been drawn in Fig. 5, but they are trivial and have been ignored for ease of drawing.)

Figure 4 has, clearly, only one other face besides the one whose boundary is shown in Fig. 5. Thus $F = 2$, and the number of handles is $\frac{1}{2}(2 + 6 - 4 - 2) = 1$.

The number of boundaries b in Fig. 4 is one, because only one of the two lines that define the two faces encounters external lines. In general b is the number of "face lines" that encounter external lines.

Counting the faces is trivial for a graph G that corresponds to a product of ring functions. This is because the rule that defines the topological character of G specifies that G be imbedded on the surface S in a way such that the lines coming into each vertex have the cyclic order specified by the ring function corresponding to that vertex. In the case normally considered in graph theory the cyclic order in which the lines should come into a vertex, when G is imbedded in S , is not given beforehand. Thus one must, in principle, try each possible combination of cyclic orderings at the various vertices, in order to find which one gives, via the procedure shown above, the maximum number of faces F , and hence, by formula (1.1), the minimum number of handles h . This procedure of trying each combination of cyclic orderings of the lines at each vertex is precisely Youngs' algorithm for computing the genus of a graph. But in

our case the ordering corresponding to each vertex is specified, and hence there is only one set of orderings to consider. The calculation is, therefore, trivial.

An equivalent rule for computing the genus could be stated in terms of quark lines, but these lines have not been introduced into the theory at this stage. We see here rather an indication of how quark lines will come out from purely topological considerations.

Now that the algorithm has been given for computing h and b for any product of ring functions, one may define the topological expansion. It is assumed that the scattering function will be defined in terms of various discontinuities, and that these discontinuities will eventually be represented (formally at least) as products of ring amplitudes. Each of these products has a well-defined b and h . Thus each term is classified. It is then assumed that the connected scattering function breaks into a sum of terms:

$$(1.2) \quad S_c = \sum_{b,h} (S_c)_h^b .$$

Since each term $(S_c)_h^b$ of S_c is classified in terms of the classification of its discontinuities one must demand that the standard discontinuity formulas derived from unitarity,⁹

$$(1.3) \quad \text{disc } S_c = S_c^1 \otimes S_c^2 ,$$

should decompose in accordance with the number of boundaries and handles:

$$(1.4) \quad \text{disc } (S_c)_n^b = \left[S_c^1 \otimes S_c^2 \right]_h^b .$$

The crucial property of the theory, which is what makes the ordered Hilbert space idea useful, is that if S_o^1 is identified with the planar amplitude constructed from the ring functions defined by the ordered Hilbert space equations, then the lowest-order contribution to (1.4), namely

$$(1.5) \quad \text{disc } P = \left[P^1 \otimes P^2 \right]_o^1$$

is automatically satisfied by virtue of the discontinuity formulas satisfied by the ring functions by virtue of their unitarity property in the ordered Hilbert space. This property is not immediate because the unitarity equation (1.3), and the consequent equations (1.4) and (1.5), are formulated in the ordinary Hilbert space, whereas the unitarity properties of the ring functions are formulated in the ordered Hilbert space. However, the algorithm for calculating h and b is such that the planar ($h = 0$, $b = 1$) part of equation (1.4), is satisfied by virtue of the definition of P as a sum of ring amplitudes together with the discontinuity formulas for the ring amplitudes that follow from the ordered Hilbert space unitarity.

The validity of (1.5) is illustrated for the simplest case of a two-particle discontinuity of a two-particle scattering function by the diagrams of Figures 6 through 10, as elaborated by their captions,

This very brief description of the work of Chew, Lucht, and Weissmann is needed to pose the problem considered in this paper. That problem is to extend their ideas to baryons. A proposal for doing this is described in the following sections. The problem divides into several parts. The first, dealt with in Sections 2 and 3, is the problem of generalizing the concept of ring amplitudes and of the ordered Hilbert space. The second, dealt with in Section 4, is the problem of devising a satisfactory topological classification scheme. Further points are discussed in the later sections.

00104807307

2. The Ordered Amplitudes

The ordered amplitudes are assumed to include those that can be represented by surfaces that can be imbedded on spheres ($h = 0$), that have the minimum number of boundaries ($\delta = b - b_{\min} = 0$), and that have no baryon closed loops ($l = 0$). These surfaces are exactly the ones that correspond to the lowest-order amplitudes in the scheme described in refs. 10 and 11 and the notations are the same as in that paper.

The surfaces associated with these "planar" or ordered amplitudes have a simple topological structure. If the capping operation¹⁰ is not performed, so that the single surface breaks into a set of disconnected parts, called components, then each of these components is topologically equivalent to a disc with mesons and baryons attached to the boundary in a well-defined cyclic order. A typical component is shown in Fig. 11, and is drawn in two slightly different forms in Figs. 12 and 13. The dotted line is one of the three "inner lines" associated with each baryon. These three inner lines are required to stay together, and the triad, taken together, is represented as a dotted line in the baryonic quark diagram. This dotted line is called a baryon line.

Each dotted line of Fig. 11 is one of a triad of inner lines. Three components, like the one of Fig. 11, must come together at each dotted baryon line of a baryonic quark diagram. A typical arrangement of components is shown in Fig. 14. Three component sheets come together at each dotted baryon line. But they are not actually joined along this dotted line.

A channel can have a nonzero normal threshold discontinuity if the corresponding surface σ can be cut into two disjoint parts each of which is connected and contains precisely one of the two sets of particles that define the channel. The cut is to be drawn so that it remains outside the capping regions, and cuts either all three inner lines associated with a given baryon line or none of them. Then the cut defines a tree graph, with one edge for each component that it passes through, and one three-line vertex for each baryon line that it passes through. For example, a cut that slices through the surface of Fig. 14 in the manner shown in Fig. 15a gives the tree graph shown in Fig. 15b. This tree graph shows the shape of the interface of the two parts of σ . These interface tree graphs play an important role in what follows. This requirement that the two parts of the capped surface σ be connected entails that the cut pass through no baryon line more than once. The special status given to this class of cuts differentiates the present work from that of Ref. 10.

In the foregoing discussion each ordered amplitude was represented by a surface. However, there is an equivalent graphical presentation. Consider first the simple surface shown in Fig. 16. A corresponding graph is Fig. 17. Another corresponding graph is Fig. 18. The graphs 17 and 18 are equivalent in the sense that they are in one-to-one correspondence. One passes from graph 17 to graph 18 by removing the dotted lines. One passes from graph 18 to graph 17 by the rule: if a pair of vertices is joined by two solid lines, then join them also by a dotted line.

Figure 19 is a typical allowed diagram. One should visualize three separate sheets coming together at each dotted line. Using these dotted lines one can draw the interface tree graph corresponding to any cutting of the surface into two disjoint parts. These dotted lines are therefore important. However, they can be reconstructed from the solid lines alone. The rule is this: if two vertices are joined either by a pair of solid lines or by a pair of lines each of which is either a solid line or a solid line with one or more dotted internal segments then join these two vertices by a dotted line. Repeat this operation until no more dotted lines are added.

Every graph that corresponds to a planar or ordered amplitude can be constructed by the following procedure: start with a circle (which is what one has in the meson sector) and replace some solid segment by a set of three lines in the manner shown in Fig. 20.

Apply this procedure repeatedly. One can choose to leave out the dotted lines, since they can be reconstructed later from the solid lines when needed.

The graphs generated in this way, without the dotted lines are called necklace graphs. The idea that the ordered amplitudes for baryons should correspond to quark diagrams that are necklace graphs was arrived at by Finkelstein and Weissmann via arguments quite different from those used in the present work. The presentation of the theory in terms of necklace graphs instead of surfaces is diagrammatically simpler and will be done wherever feasible. A principal advantage of the presentation in terms of necklace graphs is that these graphs can (and always will) be drawn as planar graphs. The necklace graphs with added dotted lines connecting pairs of baryon vertices also can (and always will) be drawn as planar graphs.

807308

3. The Ordered Hilbert Space

The states of the ordered Hilbert space will be called the ordered states. The bracket product $\langle \psi_j^{\text{out}} | \psi_i^{\text{in}} \rangle$ of two ordered states must be a well-defined ordered amplitude. Thus the ordered in and out states should be represented by the two halves of the diagrams representing the ordered amplitudes.

If the surface representing an ordered amplitude is cut into two connected parts then, as mentioned in the preceding section, the interface is a tree graph. Each half of the surface is conveniently represented by a graph obtained by joining the interface tree graph to the graph formed from the solid (quark) lines that bound the half surface. Thus we write

$$(3.1) \quad |\psi_i\rangle = |F_i G_i\rangle,$$

where F_i represents the interface tree graph and G_i represents the graph consisting of the quark lines that bound the half surface. The product graph $F_i G_i$ (where the lines are joined in the natural fashion defined by original cutting) is a necklace graph.

Interface graphs that are topologically equivalent are considered identical. Thus the two graphs of Fig. 21 are identical. More generally, interface tree graphs are considered identical if with some numbering of lines and vertices they have the same incidence matrix.

Then the complete set of states $|F_i G_i^{\text{in}}\rangle$ is constructed by taking the complete set of possible interface graphs F_i , and connecting each one to all possible graphs G_i such that the product $F_i G_i$ is a necklace graph. This graph can be drawn on a plane with the F_i part standing to the left of the G_i part.

The bra vector $\langle F_j G_j^{\text{out}} |$ corresponding to a ket vector $|F_j G_j^{\text{in}}\rangle$ is represented by the mirror image of $F_j G_j$. This mirror image graph is denoted by $\tilde{G}_j \tilde{F}_j$, where \tilde{F}_j is the mirror image of F_j and \tilde{G}_j is the mirror image of G_j . Under this mirror imaging each line of a graph is taken to its mirror image, but the directions of the quark lines (in analogy to spin) are not reversed. The product $\langle F_j G_j^{\text{out}} | F_i G_i^{\text{in}} \rangle$ is zero unless $F_i = F_j$, in which case it is the amplitude represented by the graph $\tilde{G}_j G_i$.

One can visualize $F_i G_i$ attached to a right hemisphere, with F_i on the flat circular part and G_i on the hemispherical part, and $\tilde{G}_j \tilde{F}_j$ similarly attached to the left hemisphere. Then the two graphs \tilde{F}_j and F_i can be considered to cancel, leaving the graph $\tilde{G}_j G_i$ on the outer (spherical) surface. This graph $\tilde{G}_j G_i$ will be a necklace graph.

Some examples of these constructions will now be described. Figure 22 shows a typical ordered amplitude graph. It can be separated into two connected parts by the closed circle drawn as a dotted line in Fig. 22. This separation of the ordered amplitude graph into two connected parts by means of a closed circle is the graphical equivalent of cutting the corresponding surface into two connected parts.

Figure 23 shows the same graph with the dotted lines added, and with the cut through the surface shown. The associated interface tree graph is shown in Fig. 24. This graph will be called F_i . The graph formed from the solid (quark) lines on the right-hand side of the cut will be called G_i . The product $F_i G_i$ is shown in Fig. 25, with a dotted line added to show the separation between F_i and G_i . The vertices of the G_i part of the graph will be indicated with heavy dots, to indicate connections to external particles, whereas the vertices of the F_i side will not be dotted, since they show only a topological connection. The necklace graphs $F_i G_i$ that characterize states are called state graphs. They should be distinguished from the amplitude graphs that characterized the amplitudes. Every vertex of an amplitude graph has a heavy dot.

The left-hand-side of Fig. 22 yields a state graph $\tilde{G}_k \tilde{F}_k$ which is shown in Fig. 26. The interface graph F_k is the same as F_i . Placing the graphs 25 and 26 on right and left hemispheres one sees that the graphs \tilde{F}_k and F_i cancel in the sense that they have identical structures, but the arrows run in opposite directions.

The amplitude $\langle F_i G_i^{\text{out}} | F_i G_i^{\text{in}} \rangle$ corresponds to the graph $\tilde{G}_i G_i$ obtained by joining the graph of Fig. 25 to its mirror image. The amplitude $\langle F_j G_j^{\text{out}} | F_j G_j^{\text{in}} \rangle$ corresponds to the graph $\tilde{G}_j G_j$ obtained by joining the graph of Fig. 26 to its mirror image.

It is an immediate consequence of these rules that two states can couple only if they have the same interface graph F_i . In order to preserve, for ordered amplitudes, the notion of pole dominance, which is the essential idea of duality, one must have particles corresponding to each interface graph F_i . These particles should be represented by vertices with heavy dots.

But so far all vertices connect either two lines (meson vertices) or three lines (baryon vertices). However the interface diagram of Fig. 24 connects four lines. Thus four-line vertices must be introduced into the formalism. That is, dots with more than three lines must be allowed. However, each of these new dots should correspond to an interface tree graph. Thus all of the above discussion in terms of necklace graphs is preserved if one simply considers every heavy dot to have an internal structure that is an interface tree graph. Each interface tree graph continues to have only three-line vertices, and hence the necklace structure of ordered amplitude graphs is revealed when the interface tree graph associated with each heavy dot is exhibited.

0.0 1.0 4807309

4. Topological Classification of Products

A topological classification of every multiple product of ordered amplitudes is required. A product of two amplitudes means here a product of the type occurring in a unitarity sum: the particles of the two amplitudes are paired-up in some specified way, and the momentum and spin variables of paired particles are equated, and summed over all physical values.

If G_1 is one ordered amplitude graph and G_2 is another ordered amplitude graph then a particular product is represented by a one-to-one pairing of the some of the heavy dots of G_1 with corresponding heavy dots of G_2 . Such a pairing is indicated in Fig. 27.

The notion of "connecting tubes" is now introduced. Notice that the three particles a , b , and c , are linked together in the same way in G_1 and G_2 except that the arrows run in opposite directions. More precisely one can, by means of a circle, cut the graph G_1 to display a state containing precisely the three particles a , b , and c , and one can do the same thing for G_2 . These two states are represented by mirror image graphs, FG and $\tilde{G}\tilde{F}$. In such a situation the two structures G and \tilde{G} can be considered to cancel out, in the sense as was described in the preceding section, and the two spheres, carrying G_1 and G_2 respectively, can be considered to be joined by a tube that carries the uncanceled quark lines from one sphere to the other. This construction is indicated in Fig. 28 and Fig. 29. The connections e and f

of Fig. 27 cannot be combined with anything else, and hence require separate connecting tubes. Thus the topological structure associated with the product indicated in Fig. 27 is two spheres connected by three tubes. The genus of this surface is 2. Thus this product is classified as $\gamma = 2$.

Each tube corresponds to a pair of mirror image states $|F_1 G_1\rangle$ and $\langle F_1 G_1|$. Thus each tube is characterized by a unique interface graph F_1 . As the energy flowing along the tube increases more states with this same interface graph open up. The tube can carry any one of these states, and it is considered to represent this entire set of states. Thus, the tube can be considered to represent a reggeon in the direct channel. This reggeon is characterized by the interface tree graph F_1 associated with the tube. The reggeon (or tube) can be considered to be a surface whose cross section is the associated tree graph F_1 .

Consider now an arbitrary product of two ordered amplitudes.

Each ordered amplitude is represented by a necklace graph that can be placed in a locally planar way on a sphere. The unitarity-type product of the two amplitudes is represented by making a one-to-one correspondence of certain vertices on one sphere with their mates on the other sphere. This correspondence is represented by wiggly lines, as in Fig. 27. The connecting particles can then be grouped into disjoint sets so that for each such set Γ the following condition holds: A circle can be drawn on each sphere so that (1) each of the two circles divides the ordered amplitude graph on its sphere into two connected parts, (2) on each sphere one of the two parts defined by the circle contains precisely the set of vertices that is associated with the given set Γ of connecting particles, and (3) if G_1 and G_2 are the two original amplitude graphs, and G_1' and G_2' are the parts containing the vertices corresponding to the given set Γ of connecting particles, then G_1' is the mirror image of G_2' . Each such set Γ of connecting particles is represented by a tube that connects one sphere to the other sphere. All possible ways of grouping the connecting particles, subject to the above conditions, are considered in order

to determine the minimum number of tubes needed to connect the two spheres. This minimum number is certainly no larger than the number of connecting particles. The genus of the final surface, which consists simply of the two spheres connected by the minimal number of connecting tubes t , is $\gamma = t - 1$.

The question arises whether the separation of the connecting particles into the minimum number of sets satisfying the above requirements is unique. The answer is no. A simple counter example is shown in Figs. 30 and 31.

The genus γ has a simple interpretation: it is the minimum number of reggeon closed loops associated with the surface. Each tube represents a direct channel reggeon that is characterized by the interface tree graph F_1 carried by the tube. Two tubes are called "adjacent" if (1) on each end the two circles that define these two tubes can be enlarged, by including some interior segments of lines, into a single circle that again defines a state, and (2) the states thus defined at each end are represented by mirror image graphs \overline{FG} and GF . In such a case the two adjacent tubes can be combined into a single tube that can be considered to carry from one sphere to the other a surface whose cross section is the common tree graph F . By combining adjacent tubes one can reduce the number of tubes that connect the two spheres. The genus γ is $t - 1$, where t is the minimum number of connecting tubes. If the various connecting tubes are represented as reggeon lines joined together at the spheres, and if the external particles are also

00004807310

placed on tubes corresponding to reggeons then one obtains a reggeon graph, and γ is the number of independent closed loops in this reggeon graph. In other words, γ is the Betti number of any minimal reggeon graph associated with the original surface, where a minimal reggeon graph is a reggeon graph with a minimal number of independent closed loops.

In the general case one has a unitarity-type product of many ordered amplitudes. Each of these ordered amplitudes is represented by a surface. To obtain an unambiguous topological classification one must use the reggeized form. Then each particle connection between two surfaces becomes a (reggeon) connecting surface that has as its cross section an associated interface tree graph. Each external particle is connected to the surface associated with a single ordered amplitude. It is also reggeized and hence is also represented by a surface whose cross section is a tree graph. Each original ordered amplitude is thus a surface that joins together a set of reggeon lines. Each of these reggeon lines is associated with a tree graph, and the various tree graphs corresponding to the set of reggeons that are connected by the surface corresponding to an ordered amplitude fit together to form a necklace graph. This necklace graph is the reggeon representation of the ordered amplitude. The complement in each of these necklace graphs of the tree graph representing any one of the incident reggeons must be a connected graph.

Starting from this original reggeon graph one tries in all possible ways to reduce the number of closed reggeon loops by combining adjacent reggeons, which are reggeons represented by adjacent tubes. The minimum number of closed reggeon loops is γ . Further discussion is given later.

Each reggeon surface is characterized by the number γ described above, and also by the number $\delta = b - b_{\min}$, where b is the number of boundaries and b_{\min} is a certain minimum number of boundaries.

The number of boundaries b is computed in the manner discussed in the preceding paper. That rule translates into a simple procedure in the graphical presentation used in this paper.

The advantage of the graphical presentation is that the planar amplitudes can be represented by planar graphs. The planar graph corresponding to a planar amplitude is in fact unique, apart from transformations arising from the fact that the graphs are really graphs on a sphere that are merely displayed on a plane. A simple example of three equivalent planar graphs is shown in Fig. 32. In general one can slip lines around the back of the sphere and bring them into position on the other side of the planar presentation.

The planar graphs are drawn on a plane, in a manner such that their lines (both solid and dotted) do not cross. This places a restriction on the ordering in which the three quark lines come into the baryon and antibaryon vertices: the cyclic ordering in which the quark lines come into a baryon vertex V is correlated to

the cyclic order in which the three quark lines leave the anti-baryon vertex \bar{v} that is connected to v by a dotted baryon line. This correlation is illustrated in Fig. 33.

Because of this correlation the rule for tracing face lines given in the preceding paper becomes simple in the graphical presentation. The original rule was that each quark line that enters a baryon vertex v is continued, first along the dotted line to \bar{v} and then along the outgoing quark line that forms part of the boundary of the same surface, where the three surfaces near the baryon line are the three surfaces that come together along the baryon line. In the graphical presentation this rule becomes the simple rule illustrated in Fig. 34. The graphical rule is that if the quark line enters the baryon vertex v next to the dotted line then the continuation from \bar{v} is along the quark line that leaves \bar{v} on the same side of the dotted line. This rule determines how two of the three quark lines continue through the dotted line. The continuation of the remaining quark line is thus also determined: if the incoming quark line at v is not adjacent to the dotted line then its continuation at \bar{v} is via the outgoing quark line that is not adjacent to the other end of the dotted line.

5. Formula for γ

Consider first the meson sector. Then a typical product is represented in Fig. 3. The four solid circles represent the four ordered amplitudes, and the wiggly lines are now the reggeons, which can be either external or exchanged. In a pure reggeon diagram the solid circles are contracted to points.

The formula for γ in the pure meson sector is

$$(5.1) \quad \gamma = 1 + E - V - W,$$

where W is the number of simple windows in the pure reggeon diagram. A simple window is a planar window: it is a window that can be drawn on a plane without crossing itself.

If one writes

$$(5.2) \quad F = b + w$$

where b is the number of boundaries and $w = W + W'$ is the number of windows, then Euler's formula

$$(5.3) \quad 2h = 2 + E - V - F$$

gives

11 3 7 0 4 8 0 7 3 1 1

$$(5.4) \quad 2h + b - 1 = 1 + E - V - W - W',$$

which can be compared to γ . The difference W' is the number of nonsimple windows.

Formula (5.1) is derived by starting with the Betti number

$$(5.5) \quad \beta = 1 + E - V$$

of the original pure reggeon diagram. It is the number of independent closed loops in the original diagram. One then subtracts the number W of simple windows to give

$$(5.6) \quad \gamma = \beta - W.$$

The number W is subtracted off because each simple window can be contracted out by fusing adjacent reggeon lines, and conversely each fusion of adjacent reggeon lines eliminates a simple window.

The above derivation applies immediately to the product of just two ordered amplitudes. If a simple window occurs in the graph representing any product of two ordered amplitudes then there are two adjacent reggeons in the diagram that can be fused into a single reggeon. This is illustrated in Fig. 36. In that diagram the two center exchanged reggeons can be placed on a single tube, in accordance with the rules described in section 4. They are

thereby fused into a single reggeon. On the other hand, if there is a pair of adjacent reggeons that can be placed on a single tube, and hence fused into one, then they must be separated by a simple window and this window will drop out when these two reggeons are fused. Thus $\gamma = \beta - W$ is the number of independent loops that will be left when all sets of adjacent reggeons are fused.

Figure 37 shows a diagram that is equivalent to the one of Figure 36 with respect to the number of boundaries b and the number of handles h . However, $\gamma = 2$ for Fig. 36, but $\gamma = 3$ for Fig. 37. The usual quark line structures corresponding to Figs. 36 and 37 are shown in Fig. 38 and 39, respectively. Although both structures have $b = 1$ and $h = 1$ their structures are very different, since Fig. 38 has the handles on the boundary line whereas Fig. 39 has the handles on the window. Thus this window cannot be collapsed to a point and removed from the surface in the familiar way.

Comparing the formulas

$$\gamma = 1 + E - V - W = \beta - W$$

and

$$2h + b - 1 = 1 + E - V - w = \beta - w$$

one sees that in the latter the total number of windows is subtracted from β whereas in the former it is only the number of simple windows that is subtracted.

The rule that defines adjacent reggeons was specified in Section 4 only for diagrams that represent products of two ordered amplitudes. A coherent generalization of the earlier rule must therefore be supplied.

In the reggeon diagrams representing products of two ordered amplitudes each simple window corresponds to a simple window also in the associated quark line diagram. This correspondence was illustrated in Figs. 36a and 38. In products of two ordered amplitudes each simple window was removed by fusion of adjacent reggeon lines. An analogous treatment of a product of four ordered amplitudes is illustrated in Fig. 40. And a similar treatment of a product of six ordered amplitudes is shown in Fig. 41. These examples suggest that the natural generalization of the earlier rules to products of more than two ordered amplitudes is to again fuse together the reggeons on the periphery of each simple window. Then each simple reggeon window becomes replaced by a reggeon star graph, in the manner indicated in Fig. 42. This rule entails that the number of independent closed loops is again reduced by the number of simple reggeon windows and hence $\gamma = \beta - W$ as before. Thus (5.1) becomes the general formula for the meson sector.

In the baryon sector an analogous formula can be obtained, provided the number ℓ of baryon closed loops is equal to zero.

Consider first a product of two ordered amplitudes. Each of the ordered amplitudes is represented by a necklace graph. Each reggeon that is incident upon the necklace is represented by a tree graph that can be cut out of the necklace graph by a circle. A reggeon is incident upon an ordered amplitude, or upon the necklace graph that represents it, if and only if the complement in the necklace graph of the tree graph associated with the reggeon is connected. This property stems from the connection of the ordered amplitudes to the ordered Hilbert space.

Originally there is some set of reggeons exchanged between the ordered amplitudes. Two of these reggeons are adjacent only if at each end the two circles that define the two tree graphs corresponding to the two exchanged reggeons can be enlarged, by including some lines of the necklace graph that run between them, into a single circle that defines a new reggeon that is incident upon the necklace graph. The new reggeons formed in this way at the two ends must be the same reggeon. That is, they must be associated with the same tree graph F . In this case the two original exchanged reggeons are said to be adjacent, and they can be fused together to make the new reggeon with tree graph F .

0.0 0 4 8 0 7 3 1 2

An important feature of the situation in the baryon sector is illustrated in Figs. 43 and 44. In Fig. 43 two baryon tubes connect the necklace graphs that represent the two ordered amplitudes. If a fusion of these two tubes is attempted on the left-hand-side then the tree graph for the fused reggeon would be the tree graph F_2 with two vertices and five lines. If fusion is attempted on the right-hand-side then the tree graph for the fused reggeon would be the tree graph F_0 with zero vertices and one line. These two tree graphs are not the same, and hence the two exchanged reggeons cannot be fused into a single exchanged reggeon.

The difference between tree diagrams corresponding to the fused reggeons on the right and left arises from the incidence requirement. This incidence requirement is stated without reference to the dotted lines. However, its effect is to demand that two reggeons can be fused only if their connections via dotted lines is the same on the right- and left-hand sides. That is, if two reggeons are to be fused, then any pair of junction lines that runs between the two necklace graphs must be joined together either at both ends or at neither end by the dotted lines that can be added (unambiguously) to the two necklace graphs. If the connections via dotted lines is different at the two ends then the tree diagrams at the two ends will not match, and the two reggeons cannot be fused into a single one.

The expression for γ when baryons are present, but no baryon closed loops are present ($l = 0$) is

$$(5.7) \quad \gamma = \hat{\beta} - W,$$

where $\hat{\beta}$ is the Betti number of the graph \hat{G} described in the preceding paper and W is again the number of simple windows. However, the interior face-lines of tadpole diagrams of the type shown in Fig. 45 should not be counted as simple windows because the associated reggeon loop cannot be contracted out, for the reasons described in the preceding paragraph.

An example is given in Fig. 46 and 47. The graph \hat{G} associated with the joined surface $\hat{\sigma}$ indicated in Fig. 46 has three components. One has no closed loop, the second has one closed loop, and the third has two closed loops. The joining of these surfaces produces no additional closed loops. The graph has no simple windows, hence (5.7) gives $\gamma = 3$. This agrees with the fact that it has four connecting tubes, none of which are adjacent:
 $\gamma = t - 1 = 3$.

7. Conclusions

The demand for compatibility with the basic properties of the ordered S-matrix approach to the topological expansion leads to a classification of amplitudes in terms of the set of numbers (γ, δ, ℓ') , where γ is the minimum number of reggeon closed loops in the surface that represents the amplitude, and ℓ' is the number of ^{twisted and half-twisted} baryon closed loops. Each reggeon of the theory is characterized by a tree graph, each vertex of which joins exactly three lines. The three simplest tree graphs of this kind are the single line that represents a meson-type reggeon, a tree of Y shape that represents a baryon-type reggeon, and a tree of X shape that represents a baryonium-type reggeon. In the lowest order ($\gamma = \delta = \ell' = 0$) term there is no coupling between reggeons of different types, and hence baryonium cannot decay into mesons, etc.

The vertices at which several reggeons meet are represented by necklace graphs, and a set of reggeons can be incident on a vertex only if the various tree graphs corresponding to the reggeons fit together to form the necklace graph. Moreover, the complement in the necklace graph of the tree graph corresponding to any reggeon incident upon it must be a connected graph.

I would like to thank Professor G. F. Chew, Dr. F. J. Capra, Professor J. Finkelstein, Dr. J. P. Sursock, and Mr. G. Weissmann for very valuable conversations pertaining to this paper. This report describes unfinished work of the author performed at LBL, before going on a leave of absence. It is not intended for publication.

00004807313

REFERENCES

1. G. Veneziano, Nucl. Phys. B74 (1974) 365; Phys. Lett. 52B (1974) 220.
2. A. T. White, Graphs, Groups and Surfaces, Mathematics Studies 8, North-Holland, Amsterdam 1973.
3. C. Rosenzweig and G. F. Chew, Phys. Lett 58B (1975) 93;
G. F. Chew and C. Rosenzweig, Phys. Rev. D12 (1975) 3907 and Nucl. Phys. B104 (1976) 290;
C. Schmid and C. Sorensen, Nucl. Phys. B96 (1975) 209;
M. Bishari, Phys. Lett. 55B (1975) 400;
J. Finkelstein and J. Koplik, Phys. Rev. D14 (1976) 1437;
N. Sakai, Nucl. Phys. B99 (1975) 167;
Tsou S-T., Phys. Lett 65B (1976) 81;
Chan H-M., J. Kwiecinski, and R. G. Roberts, Phys. Lett 60B (1976) 367;
Chan H-M., K. Konishi, J. Kwiecinski and R. G. Roberts, Phys. Lett. 60B (1976) 476;
C. Rosenzweig, Phys. Rev. D13 (1976) 3080;
C. Schmid, D. M. Webber and C. Sorensen, Nucl. Phys. B111 (1976) 317.
4. G. Veneziano, CERN preprint TH-2311; G. C. Rossi and G. Veneziano, CERN preprint Th-2287.
5. G. F. Chew and C. Rosenzweig, Dual Unitarization: Topological Expansion, Physics Reports (To appear).
6. G. F. Chew, P. Lucht, and G. Weissmann (in preparation).
7. G. Weissmann (in preparation).

8. J. W. T. Youngs, J. of Math. and Mechanics 12 (1963) 303.
9. J. Coster and H. P. Stapp, J. Math. Phys. 11 (1970) 1441, 2743.
10. H. P. Stapp, Topological Expansion for Baryons and Mesons, Lawrence Berkeley Laboratory Report, LBL-6739.
11. K. Konishi, Baryons and Dual Unitarization, Rutherford preprint, RL-77-062/A T. 169.
12. H. P. Stapp in Structural Analysis of Collision Amplitudes, Roger Balian and David Iagolnitzer, ed. North-Holland Publishing Co., Amsterdam, New York, Oxford, 1976.

FIGURE CAPTIONS

- Fig. 1: Diagrammatic representation of a typical ring amplitude with the physical particles represented as wiggly lines. The letter R stands for ring.
- Fig. 2: Diagram showing a Landau diagram that corresponds to a singularity of the ring amplitude of Fig. 1. The wiggly lines represent physical particles. The solid circle merely defines the ring upon which the external lines meet the internal lines of the Landau diagram.
- Fig. 3: Diagrammatic representation of a typical product of four ring amplitudes. The wiggle lines represent particle connections. For each such connection there is the usual mass-shell integration over the common momentum energy vector p_i carried by that line, and a sum over μ_i . A sum over particle-types t_i could also be included in this sum.
- Fig. 4: A graphical representation of Fig. 4. Each ordered amplitude (ring amplitude) is represented by a vertex with lines representing particles entering in the specified cyclic order.
- Fig. 5: The graph of Fig. 4 with a dotted "face line". This face line indicates the boundary of a single face of $S - G$ if G is imbedded on S with each vertex locally

- imbedded on S in a way such that the lines enter the vertex in the prescribed cyclic order.
- Fig. 6: Representation of the planar amplitude as a sum of ring amplitudes. The sum is over all different cyclic orderings of the lines around the ring.
- Fig. 7: Discontinuity formula for ring amplitude $R(i,j;k,l)$ across a two-particle cut associated with particles m and n . The superscripts 1 and 2 indicate the appropriate sheets.
- Fig. 8: The discontinuity formula for the physical scattering function $S_c(1,2;3,4)$. The plus sign indicates the physical the physical sheet. The letter 1 indicates the sheet reached from the physical sheet by going counter clockwise around the (m,n) threshold. The two sheets specified by the superscripts on R^1 and R^2 are defined in the same way.
- Fig. 9: The planar part of the discontinuity formula represented in Fig. 8. If one substitutes Fig. 6 into Fig. 9, then on the left-hand-side four terms will contribute. These are the first four terms of Fig. 6. The last two terms do not have the $(1,2) \rightarrow (3,4)$ discontinuity.
- Fig. 10: Substitution of Fig. 6 into the right-hand-side of Fig. 9 gives terms of various topologies, some of which are shown in this Figure. Most combinations have $h = 0, b = 2$. Only four have $h = 0, b = 1$. These four are equal, term

0:0 0 0 4 8 0 7 3 1 4

by term, to the four surviving terms on the left-hand-side of Fig. 9 by virtue of the relations represented in Fig. 7, which originate in the ordered Hilbert space unitarity.

- Fig. 11: A typical component of a surface associated with a planar ($h = 0, \delta = 0$) or ordered amplitude. All lines are directed in the same way around the periphery. A vertex with a solid (quark) line on each side represents a meson. A vertex with a solid line coming in and a dotted line going out represents (one third of) a baryon. A vertex with a dotted line going in and a solid line going out represents (one third of) an antibaryon. The baryon and antibaryon linked by a dotted line are called a "linked pair." Vertices with dotted lines coming in and going out do not occur.
- Fig. 12: The component shown in Fig. 11, but with the mesons now represented by pairs of oppositely directed quark lines.
- Fig. 13: The component shown in Fig. 11, but with the particles now shown as wiggly lines.
- Fig. 14: Three separate components (separate surfaces) come together at each dotted line.
- Fig. 15: The tree diagram property of any surface that corresponds to an ordered amplitude ensures that the graph that lies at the interface of any cutting of the diagram into two connected parts is a tree graph. Each line corresponds

to a cut through a component. Each vertex corresponds to a cut through a dotted (junction) line. Thus three lines meet at each vertex of any interface tree graph.

- Fig. 16: A simple surface that corresponds to an ordered amplitude.
- Fig. 17: A graph with dotted lines that corresponds to the surface of Fig. 16.
- Fig. 18: A graph without dotted lines that corresponds to the graph of Fig. 17.
- Fig. 19: A typical graph (with dotted lines) that corresponds to an ordered amplitude.
- Fig. 20: Replacement of a line segment by a combination of two solid line segments and a dotted line segment.
- Fig. 21: Two identical interface tree diagrams.
- Fig. 22: A typical amplitude graph, with a dotted line showing a separation into two connected parts.
- Fig. 23: The amplitude graph of Fig. 22 with the dotted (baryon) lines added, and with the cut into two connected parts shown.
- Fig. 24: The interface graph F_1 corresponding to the separation shown in Fig. 23.
- Fig. 25: The state graph corresponding to the state $|F_1 G_1^{in}\rangle$ associated with the right-hand-side of Fig. 23.

- Fig. 26: The state graph corresponding to the state $|F_j G_j^{\text{out}}\rangle$ associated with the left-hand-side of Fig. 23.
- Fig. 27: A typical "product" of two ordered amplitude graphs G_1 and G_2 . The wavy lines connect the associated pairs of particles in G_1 and G_2 . These associated pairs are the pairs that are equated and integrated over the mass shell in the functional form of the product.
- Fig. 28: The structures of the subgraphs G_1' and G_2' associated with the sets of particles a, b, and c are displayed. These subgraphs are the parts of G_1 and G_2 that contain a, b, and c, and no other vertices, and that can be defined by separations of G_1 and G_2 , respectively, into two connected parts by means of circles.
- Fig. 29: The tube associated with the set of connecting particles (a,b,c) of Fig. 28. The quark lines that travel along the tube are the lines that enter G_1' and leave G_2' .
- Fig. 30: An example in which there are two different ways of grouping the connecting particles in order to get the minimum number of tubes $t = 2$.
- Fig. 31: The connecting lines in Fig. 30 cannot be grouped into a one set, giving $t = 1$, because if one draws the circle as in figure (a) the connectedness of the two parts of the graph is not maintained, and if one draws the circle as in figure (b) then the graph G_1' is not the mirror image of G_2' , which is shown in (c).

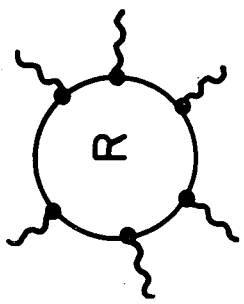
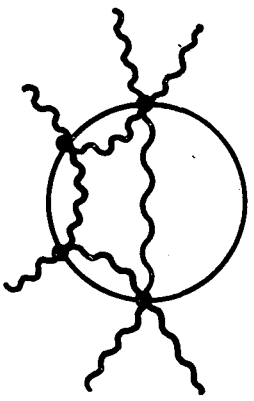
- Fig. 32: Three equivalent quark graphs. The basic quark graphs are necklace graphs that can be imbedded on a sphere. Their presentation as graphs on a plane depends on the way that the sphere is projected onto the plane.
- Fig. 33: The three components that meet at a dotted line are drawn in a planar presentation (a). In this presentation none of the solid or dotted lines cross. In the nonplanar presentation (b) some of the lines cross. The planar presentation imposes a certain connection between the cyclic orderings of the lines at v and \bar{v} .
- Fig. 34: The continuation of quark lines through the dotted lines is indicated. Incoming quark line 1 is connected to outgoing quark line 1, etc.
- Fig. 35: A typical Landau diagram that can be imbedded in the component shown in Fig. 11, the solid lines are from Fig. 11. The wiggly lines are the lines of the Landau diagram. They correspond to physical particles.
- Fig. 36: A diagram in which there is a pair of adjacent reggeons. They are separated by a simple window in the reggeon diagram. This window is removed when the two adjacent reggeons are fused into one. In this diagram $\beta = 3$, $W = 1$, and $\gamma = 2$.
- Fig. 37: A diagram that has the same number of handles h and boundaries b as the diagram of Fig. 36, but has $\beta = 3$, $W = 0$, and $\gamma = 3$.

0:0004807315

- Fig. 38: Quark line diagram representation of the diagram of Fig. 36. The simple window in the reggeon diagram of Fig. 36 corresponds to a simple window in the quark line diagram.
- Fig. 39: Quark line diagram representing the diagram of Fig. 37. There is a window, but it is not a simple window. The nonsimple window does not correspond to a pair of adjacent reggeons that can be fused.
- Fig. 40: A diagram corresponding to a product of four ordered amplitudes. The diagram has one simple window. If it is contracted out then one obtains a $\gamma = 0$ diagram.
- Fig. 41: A diagram corresponding to a product of six ordered amplitudes. It has two simple windows. If they are contracted out then one obtains a $\gamma = 0$ diagram.
- Fig. 42: Each simple reggeon window is replaced by a reggeon star graph.
- Fig. 43: Diagram representing two basic graphs connected by two tubes. The joining of quark lines along the tubes is taken to be the one that can be drawn on the plane.
- Fig. 44: Diagram illustrating why the two tubes cannot be contracted into a single tube. The contractions at the two ends give different interface tree diagrams.
- Fig. 45: A regge tadpole diagram. The interior face-line is not a simple window because it cannot be contracted out for the reason illustrated in Fig. 44. The reggeon going around the loop has, when represented by a surface, one solid (quark) line and one dotted (inner) line.

- Fig. 46: A surface with $\gamma = 3$.
- Fig. 47: Set of three reggeon graphs corresponding to three components of the surface shown in Fig. 46.

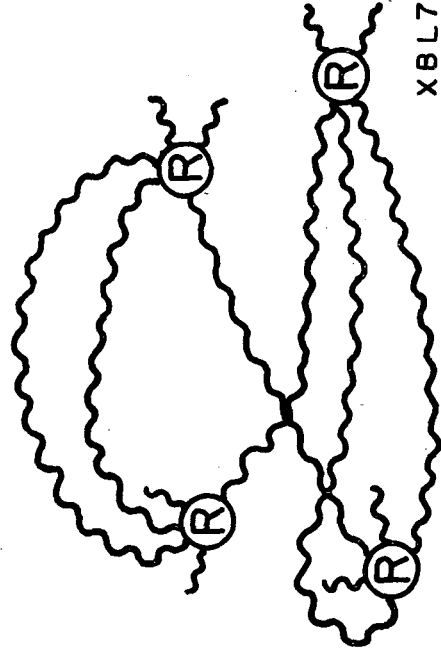
0.0004807516



XBL779-2233

Fig. 2

Fig. 1



XBL779 - 2234

Fig. 3

XBL779 - 2235

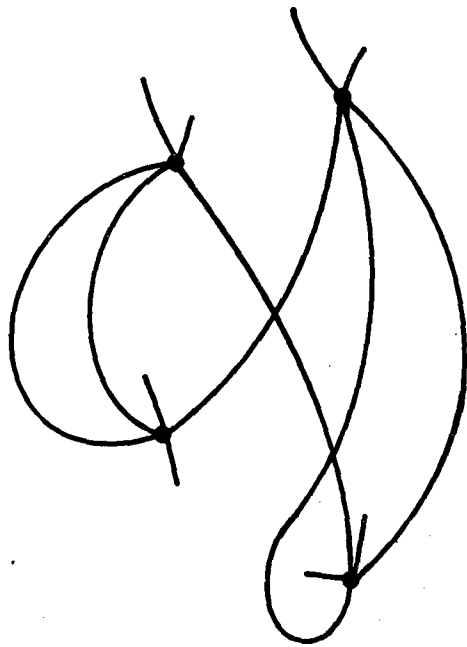
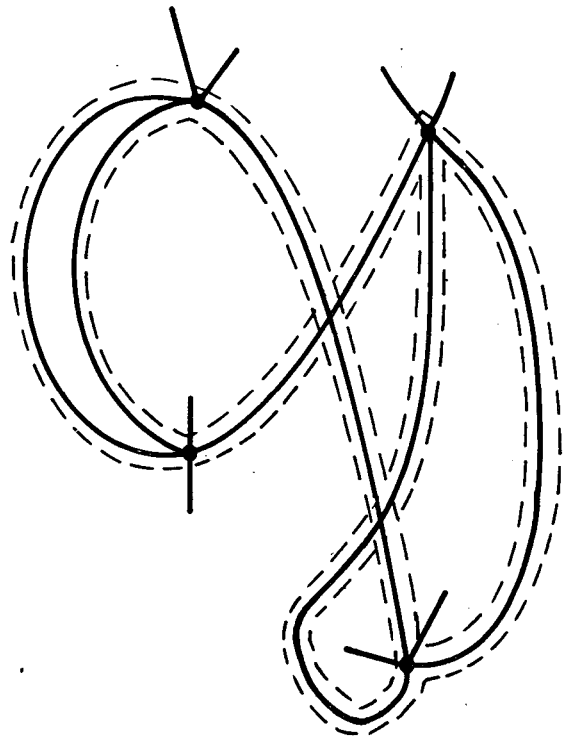


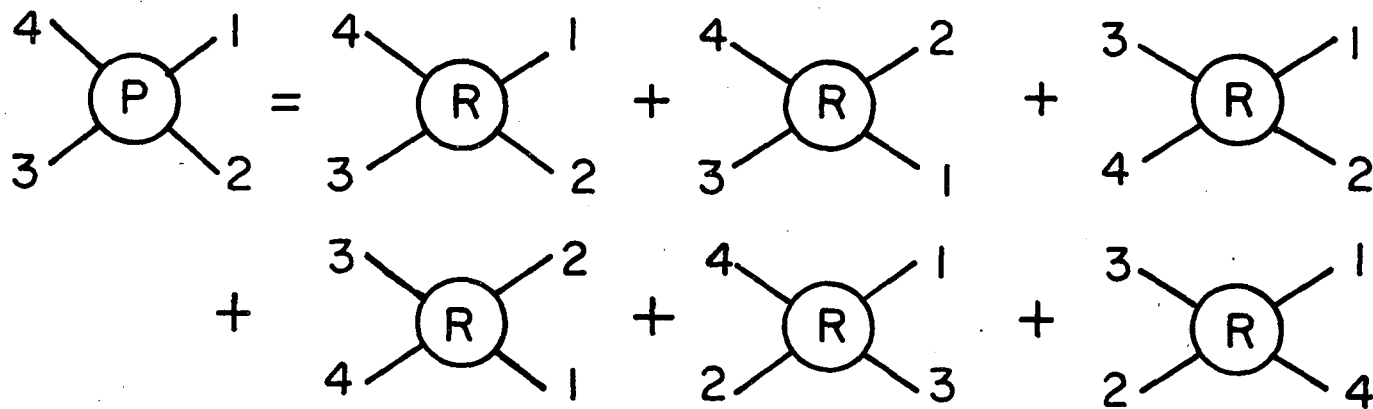
Fig. 4

00004807317



XBL779 - 2241

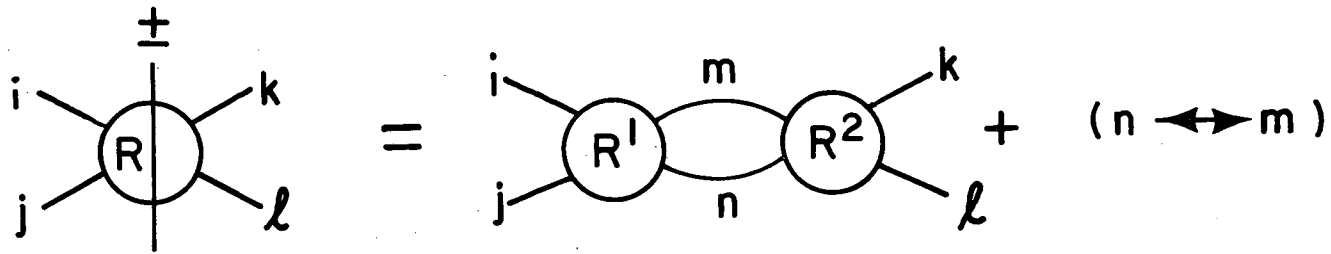
Fig. 5



XBL779 -2279

Fig. 6

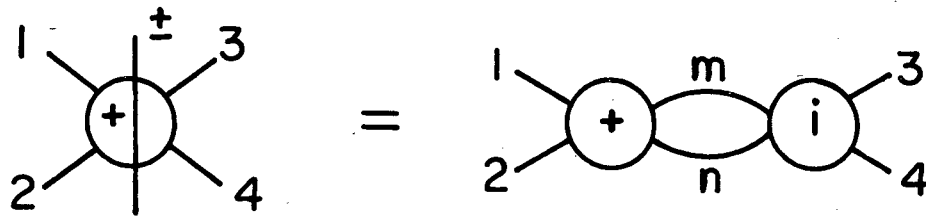
00004807518



XBL7712- 6735

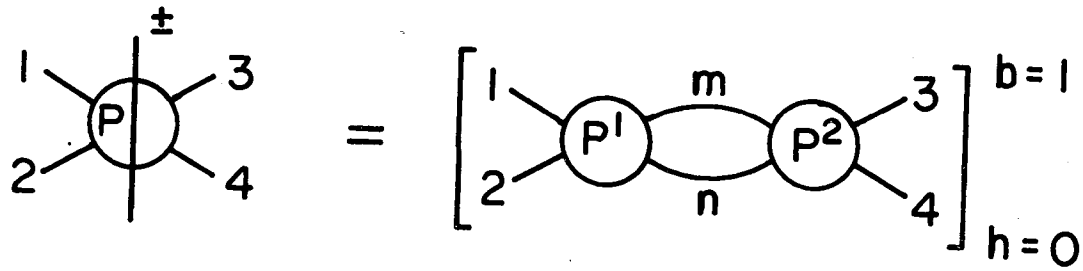
Fig. 7

0:0:0:0:4:8:0:7:3:1:9



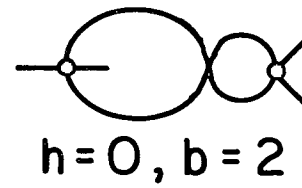
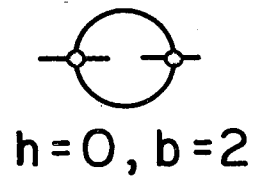
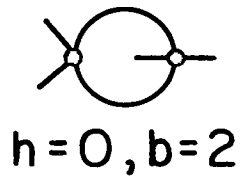
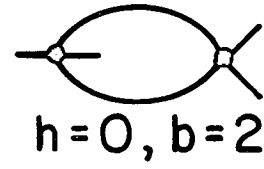
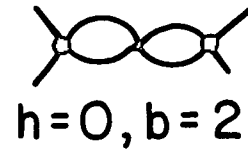
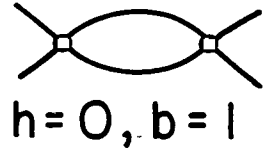
XBL779-2281

Fig. 8



XBL779-2282

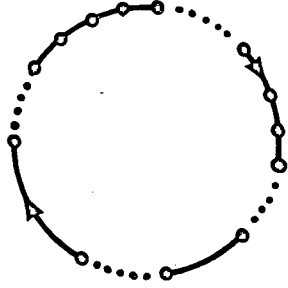
Fig. 9



XBL779 - 2221

Fig. 10

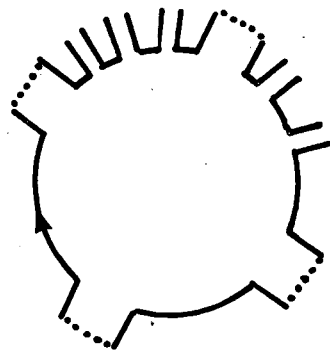
0000480/320



XBL 7710 - 6909

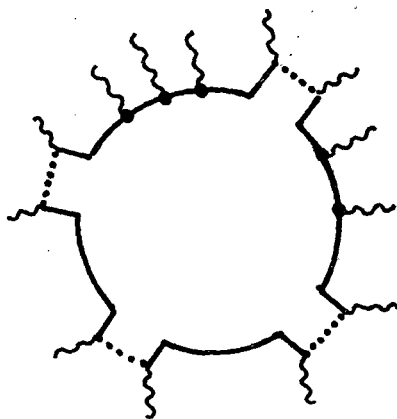
Fig. 11

... 9040480 / 321



XBL7710-6910

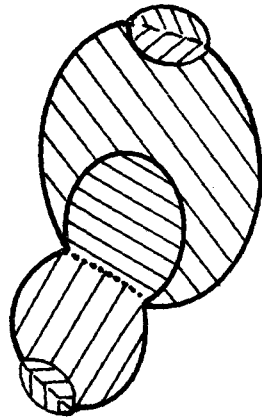
Fig. 12



XBL 7710 - 6911

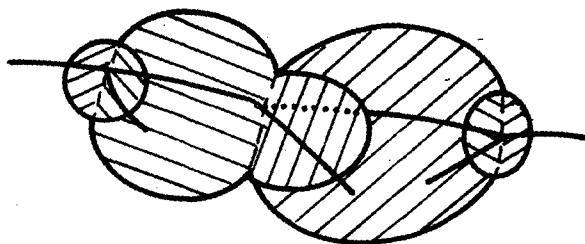
Fig. 13

00004807322



XBL779-2216

Fig. 14



(a)

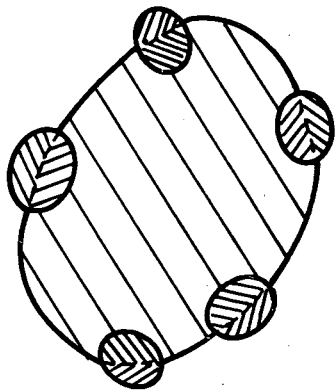


(b)

XBL779-2217

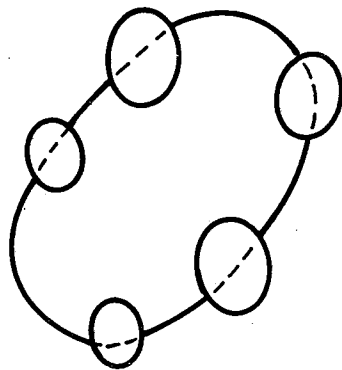
Fig. 15

00004807323



XBL779-2238

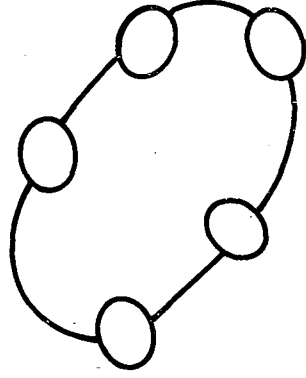
Fig. 16



XBL 779 - 2239

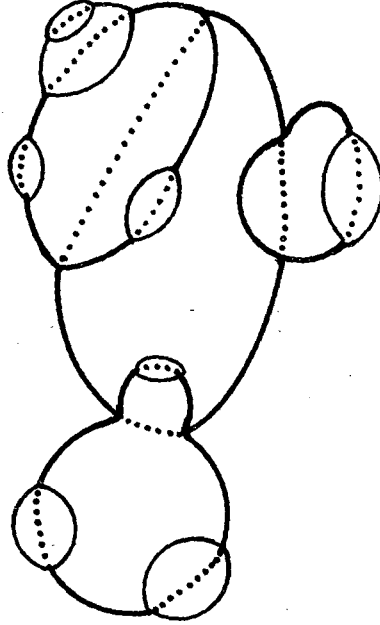
Fig. 17

004807324



XBL 779-2240

Fig. 18



XBL779 - 2228

Fig. 19

00004807325



XBL 779 - 2229

Fig. 20

XBL779 - 2225

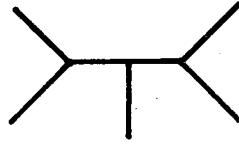
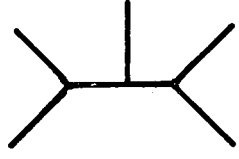
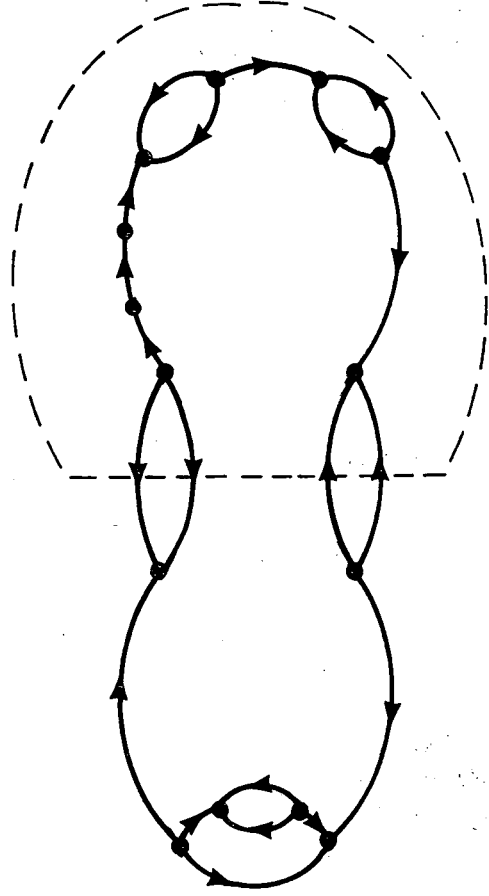


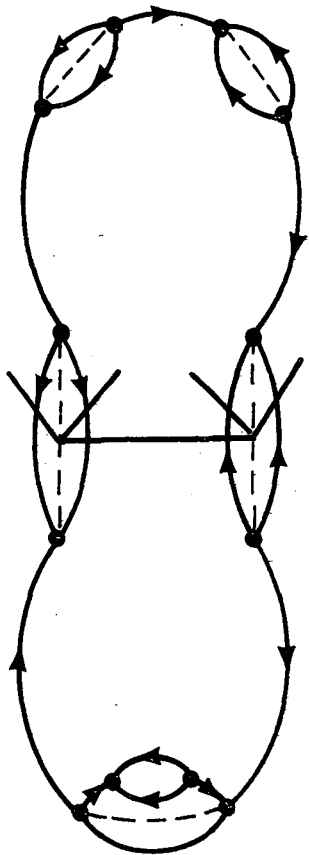
Fig. 21

00004807326



XBL779 - 2289

Fig. 22



XBL779-2290

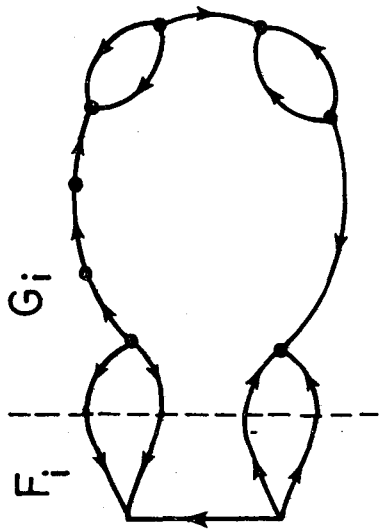
Fig. 23

00004807327



XBL779-229I

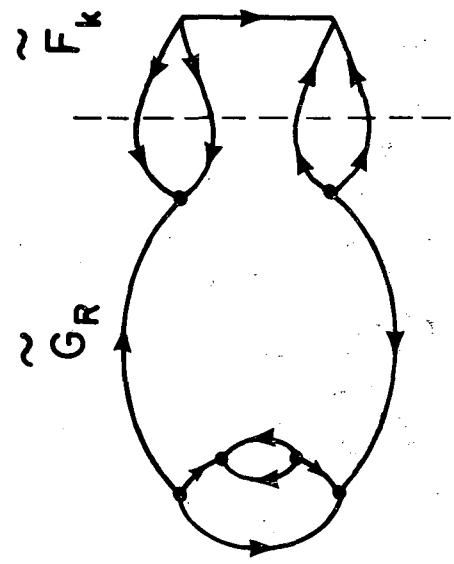
Fig. 24



XBL779-2287

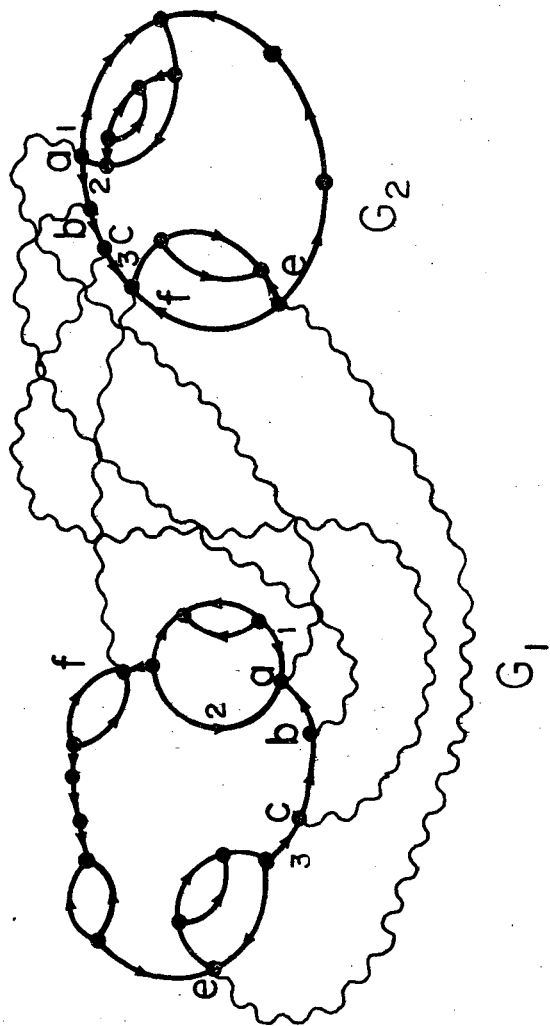
Fig. 25

00004807528



XBL779-2288

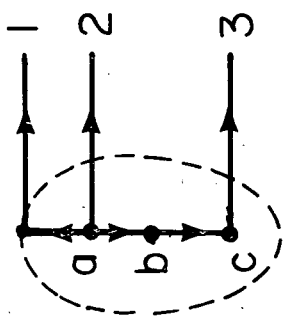
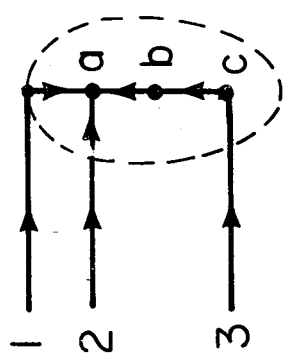
Fig. 26



XBL 779 - 2230

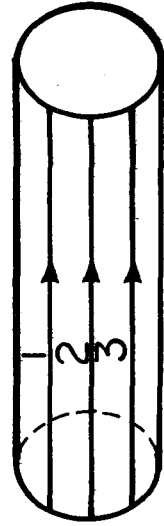
Fig. 27

00004807329



XBL779-2231

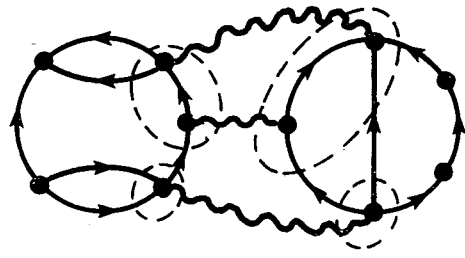
Fig. 28



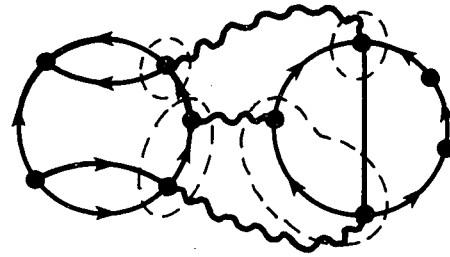
XBL 779 - 2232

Fig. 29

90004807330



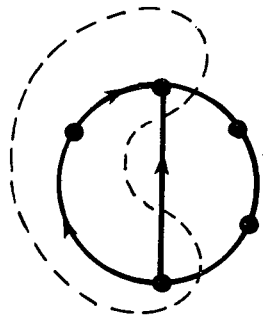
(a)



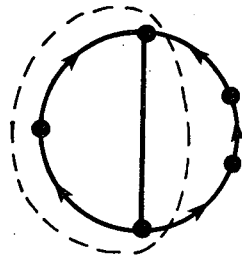
(b)

XBL779-2226

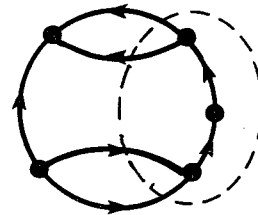
Fig. 30



(a)



(b)

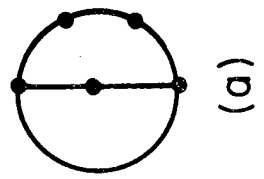


(c)

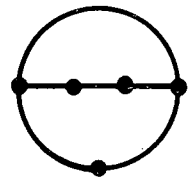
XBL779-2227

Fig. 31

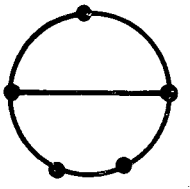
90004807531



(a)



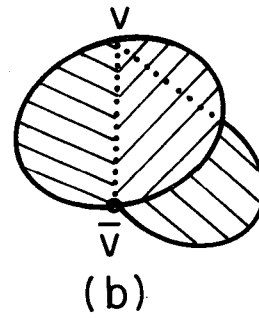
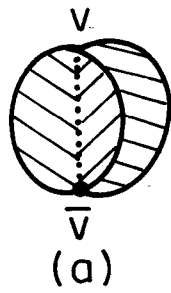
(b)



(c)

Fig. 32

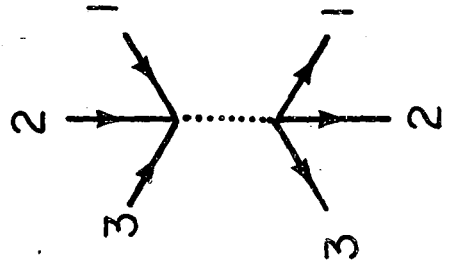
XBL779-2243



XBL779-2244

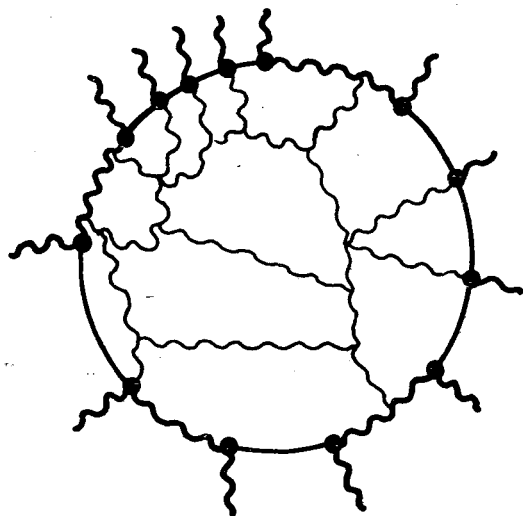
Fig. 33

98004807532



XBL 779-2245

Fig. 34



XBL779 - 2218

Fig. 35

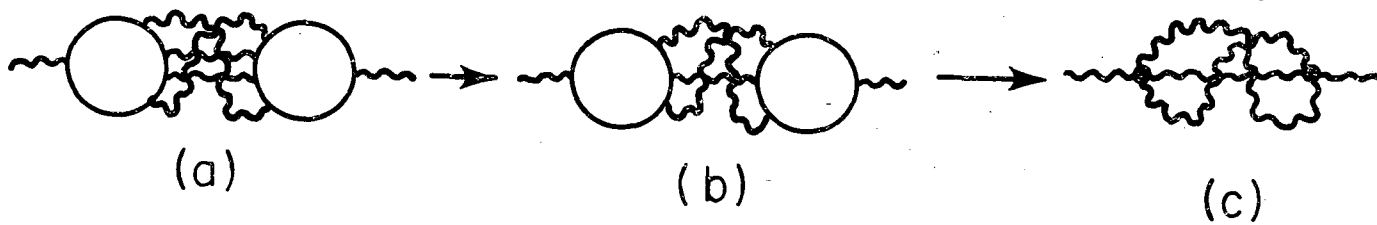
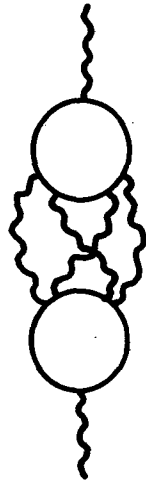


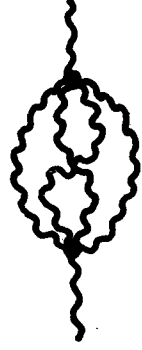
Fig. 36

XBL779-2219

90404807333



(a)



(b)

Fig. 37

XBL779-2220

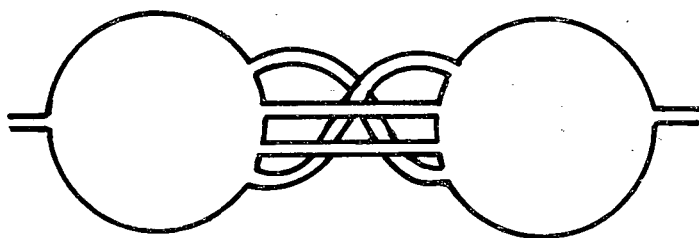
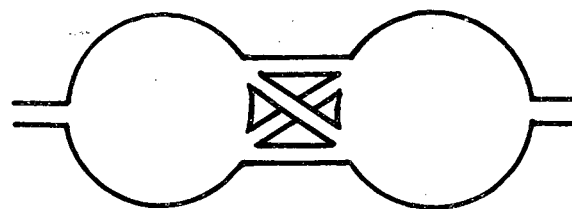


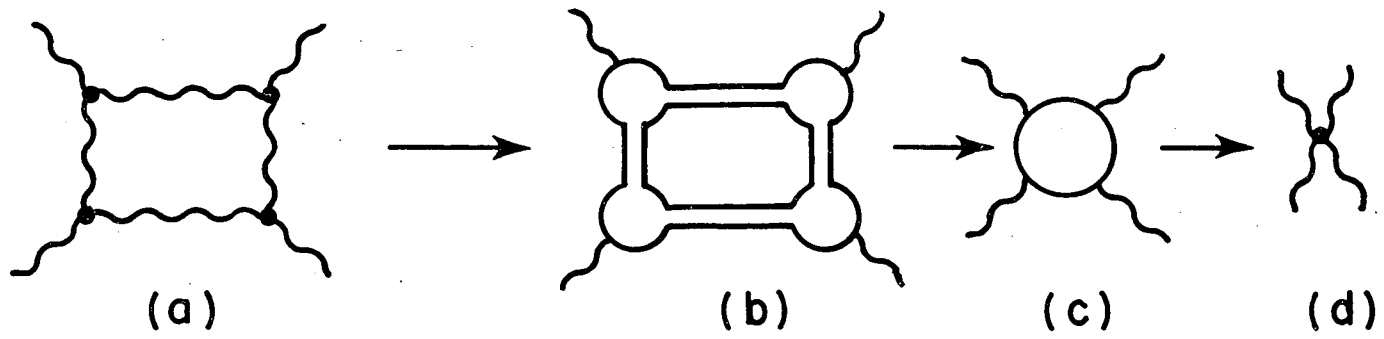
Fig. 38



XBL779-2276

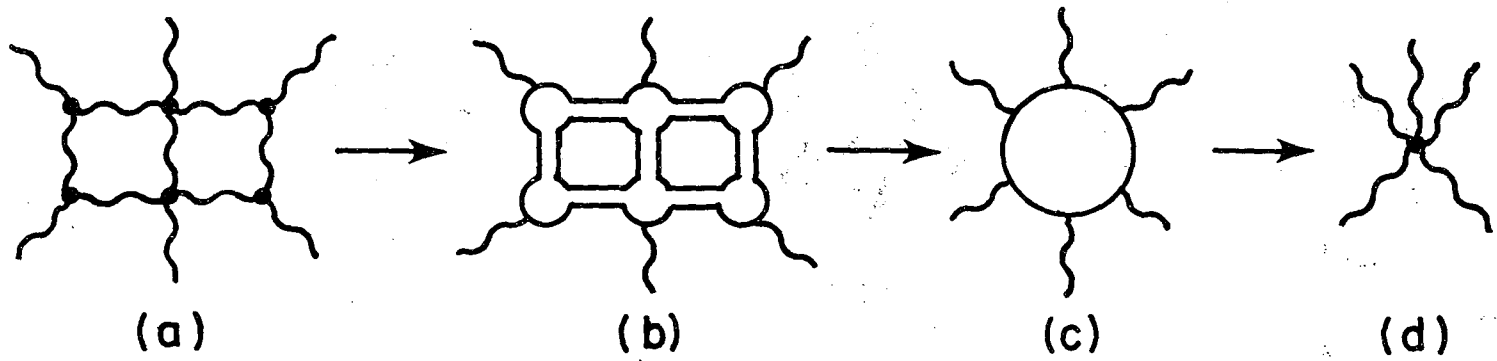
Fig. 39

9000480/334



XBL779-2277

Fig. 40



(a)

(b)

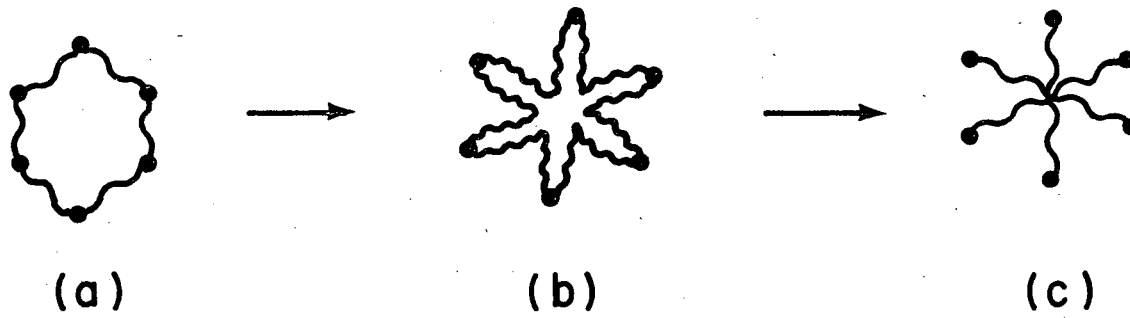
(c)

(d)

XBL779-2278

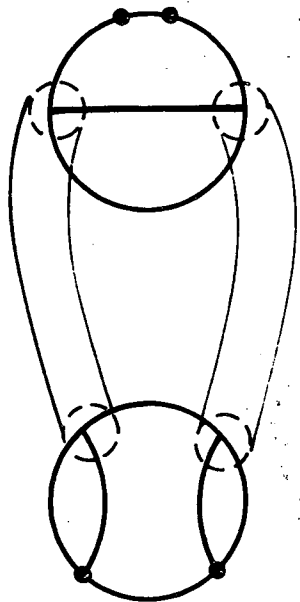
Fig. 41

00004807335



XBL779-2283

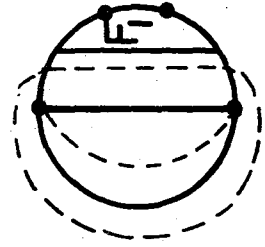
Fig. 42



XBL779-2284

Fig. 43

00404807336



XBL779 -2285

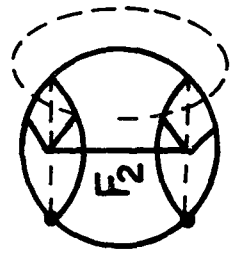
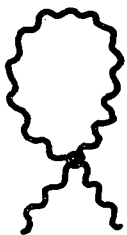


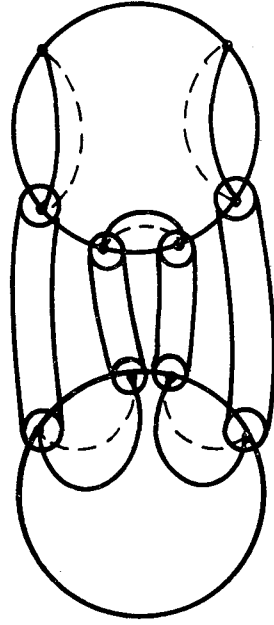
Fig. 44



XBL779-2286

Fig. 45

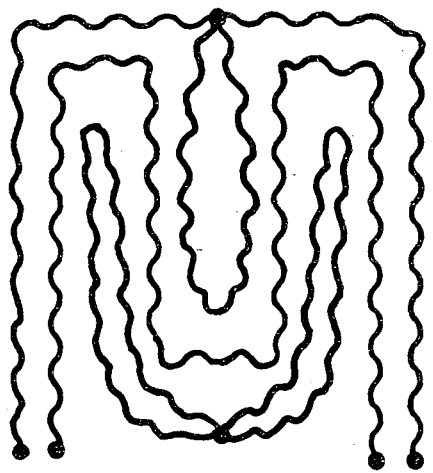
00004807337



XBL779-2237

Fig. 46

0000480/338



XBL779 - 2236

Fig. 47

This report was done with support from the Department of Energy. Any conclusions or opinions expressed in this report represent solely those of the author(s) and not necessarily those of The Regents of the University of California, the Lawrence Berkeley Laboratory or the Department of Energy.

TECHNICAL INFORMATION DEPARTMENT
LAWRENCE BERKELEY LABORATORY
UNIVERSITY OF CALIFORNIA
BERKELEY, CALIFORNIA 94720